Thrombosis Research 223 (2023) 146–154

Contents lists available at ScienceDirect

Thrombosis Research

journal homepage: www.elsevier.com/locate/thromres

Full Length Article

Plasma riboflavin fluorescence as a diagnostic marker of mesenteric ischemia-reperfusion injury in rats

Xueqin Wu [a,b,1], Lun-Zhang Guo [c,1], Yi-Hung Liu [d,1], Yu-Cheng Liu [a,b], Po-Lun Yang [c], Yun-Shiuan Leung [e], Hwan-Ching Tai [f,*], Tzung-Dau Wang [g], Jesse Chih-Wei Lin [j], Chao-Lun Lai [h,i,j,**], Yueh-Hsun Chuang [k,*], Chih-Hsueh Lin [l], Pi-Tai Chou [e,*], I-Rue Lai [d,m,***], Tzu-Ming Liu [a,b,****]

[a] Institute of Translational Medicine, Faculty of Health Sciences, University of Macau, Macau SAR, China
[b] MOE Frontiers Science Center for Precision Oncology, University of Macau, Macau SAR, China
[c] Department of Biomedical Engineering, National Taiwan University, Taipei 10617, Taiwan
[d] Graduate Institute of Anatomy and Cell Biology, College of Medicine, National Taiwan University, Taipei 10051, Taiwan
[e] Department of Chemistry, National Taiwan University, Taipei 10617, Taiwan
[f] State Key Laboratory of Molecular Vaccinology and Molecular Diagnostics, Department of Laboratory Medicine, School of Public Health, Xiamen University, Xiamen 361102, P. R. China
[g] Cardiovascular Center and Division of Cardiology, Department of Internal Medicine, National Taiwan University Hospital and College of Medicine, Taipei 10002, Taiwan
[h] Department of Internal Medicine, National Taiwan University Hospital Hsin-Chu Branch, Hsin-Chu, Taiwan
[i] Department of Internal Medicine, College of Medicine, National Taiwan University, Taipei, Taiwan
[j] Institute of Epidemiology and Preventive Medicine, College of Public Health, National Taiwan University, Taipei, Taiwan
[k] Department of Anesthesiology, National Taiwan University Hospital, College of Medicine, National Taiwan University, Taipei, Taiwan
[l] Department of Nutrition, College of Medical and Health Care, Hungkuang University, Taichung City 433304, Taiwan
[m] Department of Surgery, National Taiwan University Hospital, Taipei 100229, Taiwan

ARTICLE INFO

Keywords:
Mesenteric ischemia
Plasma fluorophores
Ultrahigh performance liquid chromatography

ABSTRACT

Due to the delayed and vague symptoms, it is difficult to early diagnose mesenteric ischemia injuries in the dynamics of acute illness, leading to a 60–80 % mortality rate. Here, we found plasma fluorescence spectra can rapidly assess the severity of mesenteric ischemia injury in animal models. Ischemia-reperfusion damage of the intestine leads to multiple times increase in NADH, flavins, and porphyrin auto-fluorescence of blood. The fluorescence intensity ratio between blue-fluorophores and flavins can reflect the occurrence of shock. Using liquid chromatography and mass spectroscopy, we confirm that riboflavin is primarily responsible for the increased flavin fluorescence. Since humans absorb riboflavin from the intestine, its increase in plasma may indicate intestinal mucosa injury. Our work suggests a self-calibrated and reagent-free approach to identifying the emergence of fatal mesenteric ischemia in emergency departments or intensive care units.

Abbreviations: NADH, Reduced nicotinamide adenine dinucleotide; FAD, Flavin adenine dinucleotide; FMN, Flavin mononucleotide; MODS, Multiple organ dysfunction syndrome; ICU, Intensive care units; AMI, Acute mesenteric ischemia.

* Corresponding authors.
** Correspondence to: C.-L. Lai, Department of Internal Medicine, National Taiwan University Hospital Hsin-Chu Branch, Hsin-Chu, Taiwan.
*** Correspondence to: I-R. Lai, Graduate Institute of Anatomy and Cell Biology, College of Medicine, National Taiwan University, Taipei 10051, Taiwan.
**** Correspondence to: T.-M. Liu, Institute of Translational Medicine, Faculty of Health Sciences, University of Macau, Macao.
E-mail addresses: hctai@xmu.edu.cn (H.-C. Tai), chaolunlai@ntu.edu.tw (C.-L. Lai), cyh771048@ntu.edu.tw (Y.-H. Chuang), chop@ntu.edu.tw (P.-T. Chou), iruelai@gmail.com (I.-R. Lai), tmliu@um.edu.mo (T.-M. Liu).
[1] Authors who contribute equally to this paper.

https://doi.org/10.1016/j.thromres.2023.01.032
Received 3 October 2022; Received in revised form 25 January 2023; Accepted 30 January 2023
Available online 3 February 2023

1. Introduction

Multiple organ dysfunction syndrome (MODS) results from uncontrolled host immune responses of cytokine storms [1] or ischemic/reperfusion injuries [2]. To facilitate the management of MODS in intensive care units (ICUs), doctors employed various medical devices and biochemical assays for the time-course monitoring of six major organ systems [3]—the cardiovascular, respiratory, renal, neurological, hematological, and hepatic systems. Based on these operational parameters of organ physiology, the sequential organ failure assessment (SOFA) score has been developed as a prognostic indicator for the clinical management of sepsis patients [4]. The gut system is not listed as the major organ in the assessment of MODS. This is partly due to the delayed & vague pathophysiological manifestation and the lack of promising biomarkers in the evaluation of gut dysfunction [5]. Besides, the intestine can tolerate hypoperfusion at 20 % of maximal blood flow [6]. The gut may still maintain normal function in the early stage of MODS or bowel ischemia. Therefore, it's hard to identify the deadly injury of the intestinal mucosal barrier in the pathophysiology of bacterial translocation, MODS [7–9], acute respiratory distress syndrome [10], and sepsis [11–13]. For severe conditions like acute mesenteric ischemia (AMI), the delayed diagnosis of intestinal necrosis can lead to very high (60–80 %) mortality [14–16]. To manage the risk of gut dysfunction in critical illness, doctors need a sensitive and easily measured biomarker to detect early injury of the intestinal mucosal barrier [17]. Evidence from medical imaging like X-ray computed tomography is usually too late to intervene.

The metabolic fluorophores or pigments in the blood are usually treated as the source of interfering background in biochemical assays. Luminescent molecules include cofactors like reduced nicotinamide adenine dinucleotide (NADH), flavin adenine dinucleotide (FAD), flavin mononucleotide (FMN), and porphyrins. Another major category of blood fluorophores is nutritional or commensal-derived vitamins like riboflavin (vitamin B_2). Since mammals cannot synthesize riboflavin, a large part of riboflavins is from dietary food, including plant foods (cereals, carrots, broccoli, collard greens) as well as animal sources (organ meats, fish, eggs, milk) [18]. Small amounts of riboflavin are produced by gut microbiota, such as *Bacteroides fragilis*, *prevotella copri*, *clostridium difficile*, *lactobacillus plantarum*, and *lactobacillus fermentum* [19]. They are predominantly absorbed from the intestine. Because the serum level of blood fluorophores is easily affected by diet, they are not considered reliable markers in cross-sectional clinical studies. But the acute systemic inflammation or cytokine storm in critical illness may injure tissues and disturb the homeostasis of metabolic fluorophores longitudinally. For example, damage-associated molecular patterns (DAMPs) [20], together with fluorescent cofactors in cells, may be released into the blood circulation and thus increases the level of blood fluorescence. The ischemic injury of the mucosal barrier in the intestinal lumen may enhance the leakage of water-soluble vitamins into the portal vein. Then the fluorescent vitamins could enter the systemic circulation via the liver. These scenarios in acute illness may lead to soaring blood fluorescence (Fig. 1a-b). In this work, we found that endogenous plasma fluorophores [e.g. NADH, porphyrin, and flavin (FAD/FMN/Riboflavin)], originally considered as interfering background, can serve as sensitive fluorescence reporters to indicate mesenteric ischemia injury in vivo and in vitro. Unlike physiological monitoring or in vitro diagnosis kits, this plasma fluorescent metabolomic approach provides a new evaluation modality in critical care medicines (Fig. 1c-d). This work paves the way for detecting mesenteric ischemia injuries in the emergency department or ICU.

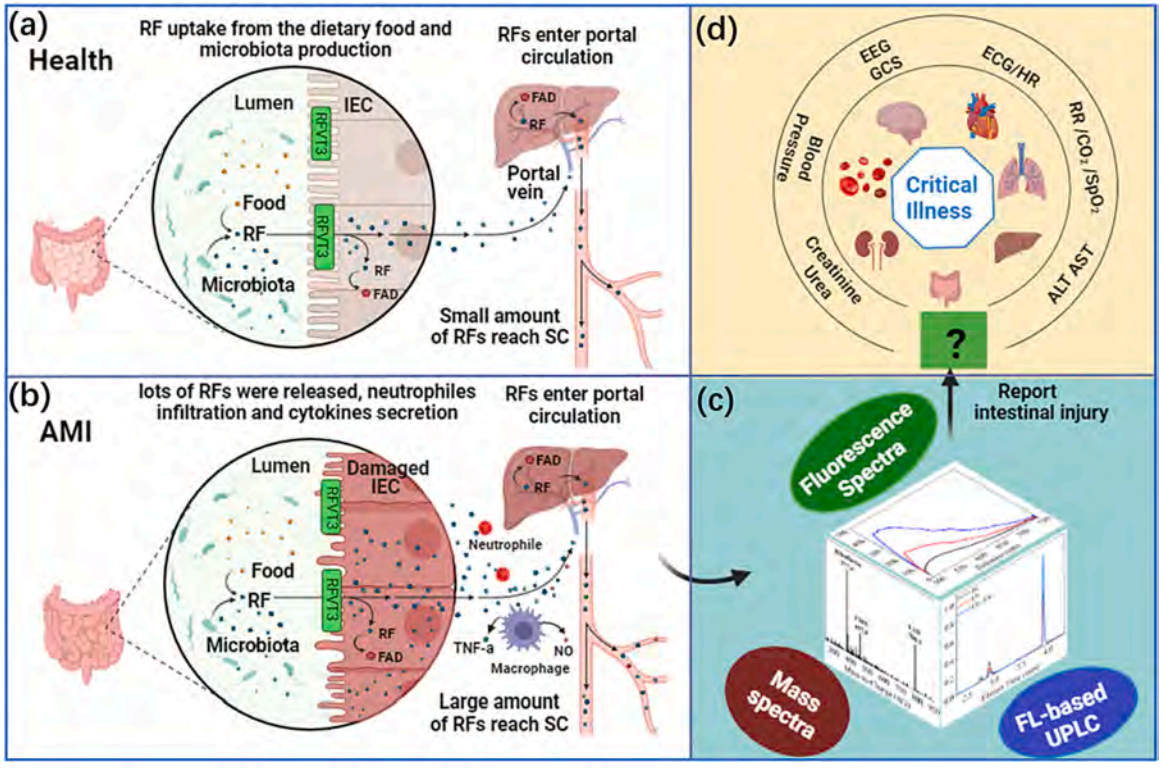

Fig. 1. (a) Riboflavin (RF) uptake and metabolism in healthy physiological conditions. Large parts of RFs are from dietary foods and small amounts of RFs are produced by gut microbiota. Partial RF is converted to FAD and stored in different organs for meeting daily needs. Small amounts of RFs finally enter the systemic circulation (SC) via the hepatic portal vein. (b) RFs uptake and metabolism under AMI condition. Damaged intestinal mucosa resulting from the mesenteric ischemia triggers neutrophile infiltration, macrophage activation, and cytokines release. The increased RFs enter SC. (c) Multi-dimensional approaches report the fatal intestinal injury in AMI; (d) Fill the gap in managing the risk of multiorgan dysfunction syndrome (MODS). IEC: Intestinal Epithelial Cells, RFVT3: Riboflavin vitamin transporter 3, NO: Nitric Oxide, EEG: Electroencephalogram, GCS: Glasgow Coma Scale, ECG: Electrocardiogram, RR: Respiratory Rate, SpO_2: Oxygen Saturation, CO_2: Carbon Dioxide, ALT: Alanine Transaminase, AST: Aspartate Transaminase.

2. Results

2.1. Acute mesenteric ischemia (AMI) increases the plasma fluorescence

In AMI experiments, the blood pressure (BP) and heart rate (HR) of rats were stable during anesthetization (Fig. S1). Under long-term ischemia-reperfusion, some rats had mild (<20 %) hypotension right after the reperfusion but gradually returned to normal. Histopathological results showed evident necrosis and immune cell infiltration in the intestine villi of 70-minute ischemia rats (O70 group), while the villi of sham rats (S70 group) were maintained intact (Fig. 2). The tissue damage hallmark, lactate dehydrogenase (LDH), significantly rose to 6.8 and 13.4 times the baseline level after 70 min of ischemia and following 30 min of reperfusion (Table 1). Besides, the plasma nitric oxide significantly increased 1.86 times over the baseline (Table 1). These results validate that our AMI model caused tissue damage and increased the free radicals in the blood.

Analyzing the excitation wavelength-dependent fluorescence spectra of rat plasma (Fig. S2), we set three excitation wavelengths to highlight three significant categories of plasma fluorophores. The 385 nm light excites blue fluorophores (λ_{max} = 445–460 nm), which may come from vitamin A1, B1 derivative, or NADH. Excitation at 405 nm could emit porphyrin fluorescence with a sharp peak of 620 nm and a broad 680 nm shoulder. The flavins' fluorescence (λ_{max} = 515–530 nm) could be selectively excited using 488 nm light. It majorly comes from FAD, FMN, and riboflavin. Their increase of concentrations in blood will lead to elevated 488 nm excited yellow fluorescence and vice versa. Although the fluorescence of bilirubin also emits at the same wavelength range as flavin, it has a much lower fluorescence quantum yield (Q.Y. = 0.001) [21] than riboflavins (Q.Y. = 0.27) and FMN (Q.Y. = 0.22) [22]. Moreover, we compared the fluorescence lifetime traces of plasma, flavins, and bilirubin (Fig. S3). We found the shorter lifetime components (τ_1) of plasma were responsible for the bound-flavin (300– 500 ps) rather than bilirubin (~125 ps) [23]. The longer components (τ_2) in BL plasma and IR plasma were ascribed to the free-FAD (2400– 2500 ps) and free-riboflavin (4800– 5100 ps), respectively (Fig. S3). The fluorescence lifetimes of the bound-flavin and free-flavin also agree well with previous literature [22]. As a result, we excluded the contribution of bilirubin in 488 nm excited fluorescence. For the background subtraction and system calibration, we used the Raman spectra of water molecules' vibration mode (v = 3400 cm^{-1}) as the internal control (Fig. S4). Under this measurement and calibration scheme, we obtained plasma fluorescence spectra of rats in groups S70 (Fig. 3a-c) and O70 (Fig. 3d-f). All the fluorescence intensities become significantly higher after 70 min of ischemia (red curves in Fig. 3d-f) and more than tripled after 30 min of reperfusion (gray curves in Fig. 3d-f). In contrast, the fluorescence levels of the sham group S70 didn't change a lot at the same time points (Fig. 3a-c).

Table 1
Nitric oxide (NO) and lactate dehydrogenase (LDH) plasma levels in rats.

Plasma level	BL (n = 10)	I70 (n = 3)	I70-R30 (n = 3)
NO (μM)	17.99 ± 3.73	24.74 ± 5.76	33.54 ± 4.28
LDH (mU/ml)	3.32 ± 0.64	22.6 ± 2.34	44.5 ± 2.05

Statistically, the baseline intensities (n = 29) of the three fluorescence bands (I_{blue}, $I_{porphyrin}$, I_{flavin}) have normal distributions with mean ± standard deviations (SD) of 121 ± 31, 7.02 ± 2.47, and 12.5 ± 3.1 kilo-counts, respectively (black boxes in Fig. 3g-i). Then, they showed a significant increase after 70 min of ischemia, and the reperfusion further [raised them 2–5 times higher] (Fig. 3g-i). The flavin fluorescence has the most prominent elevation and smallest coefficient of variation among these fluorophores.

Then, we chose flavins as in vivo indicators and performed time-course two-photon fluorescence (TPF) and second harmonic generation (SHG) microscopy excited at 920 nm (Supplementary Movie S1). As we expected, we observed a significant increase in blood fluorescence (green color) at the reperfusion after 70-minute mesenteric ischemia

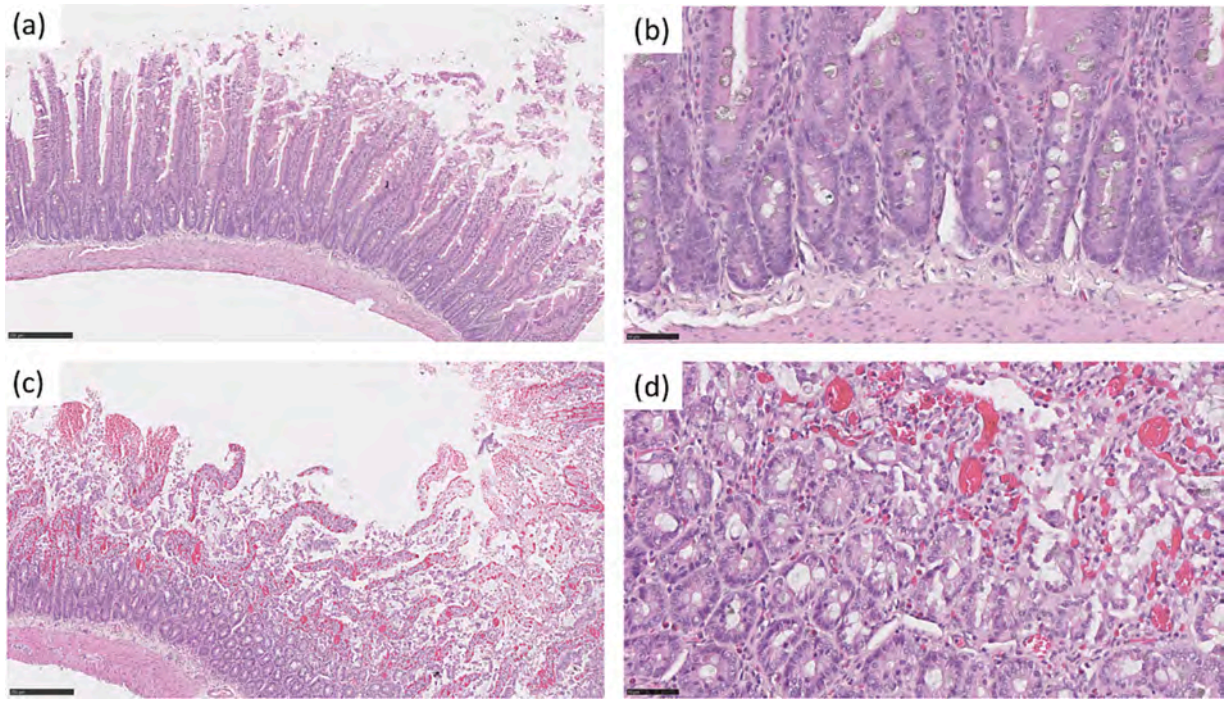

Fig. 2. Representative histological images of rat intestine: (a) Whole villi are observed in S70. Scale bar: 250 μm. (b) High power field of (a). A small amount of goblet cells and macrophages are observed in villi. Scale bar: 50 μm. (c) Villi exhibit massive necrosis, hemorrhage, and inflammatory cell infiltration in O70. Scale bar: 250 μm; High power field of (c). Disorganized necrotic enterocytes with hypereosinophilic cytoplasm and pyknotic nuclei/karyorrhexis are observed in the upper right. There are a mild number of cells: macrophages engulfing erythrocytes, eosinophilic granulocytes (eosinophils), small numbers of lymphocytes and scant plasma cells. The crypts in the lower left are mildly elongated with high mitotic activity. Scale bar: 50 μm.

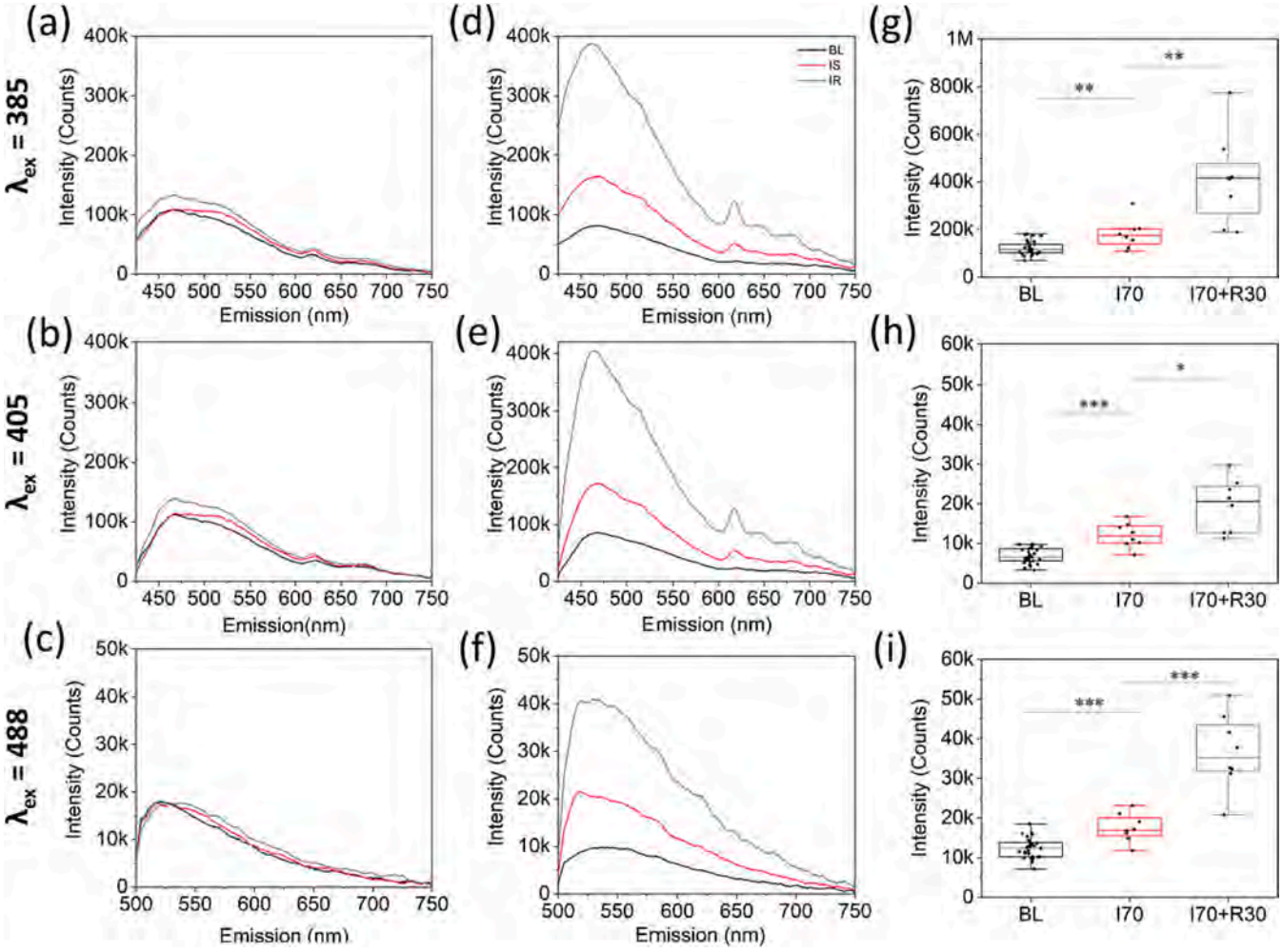

Fig. 3. Representative plasma fluorescence spectra of rats in the S70 sham group (a)-(c) and in the 70-minute ischemia-reperfusion O70 group (d)-(f). Each plasma sample was excited at 385 nm (top row), 405 nm (middle row), and 488 nm (bottom row). Three sampling time points are baseline before ischemia (BL, black curves), ischemia for 70 min (I70, red curves), and 30 min reperfusion after 70 min of ischemia (I70 + R30, gray curves). The sham group sampled the blood at the same time point without artery clamping. (g-i) Statistical plots of blue fluorescence intensity (g), porphyrin fluorescence (h), and flavin fluorescence (i) of plasma samples in 70-minute ischemia-reperfusion groups. Data points represent the fluorescence intensities of plasma in BL ($n = 29$), I70 ($n = 8$), and I70 + R30 (n = 8) samples. Mann-Whitney U test is used for hypothesis testing. Statistical significance $^{*}p < 0.05$, $^{**}p < 0.01$, $^{***}p < 0.001$. (For interpretation of the references to color in this figure legend, the reader is referred to the web version of this article.)

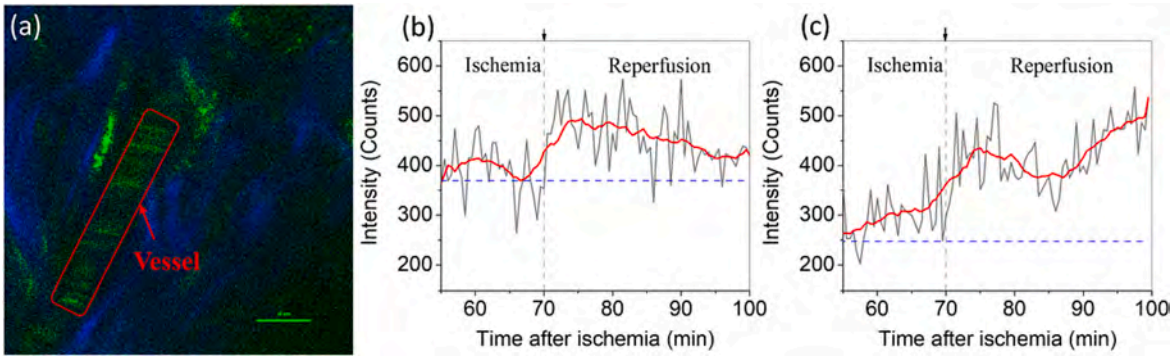

Fig. 4. (a) In vivo two-photon image ($\lambda_{ex} = 920$) mapped collagens (SHG, blue color) and yellow fluorescence (TPF, green color) in a rat's ear. Scale bar: 10 μm. (b) and (c) are time-course flavin fluorescence intensities measured from the vessel area (red rectangle in (a)) of two rats. Blue dashed lines indicate the baseline intensities of each rat. The arrows indicate the starting time of reperfusion. (For interpretation of the references to color in this figure legend, the reader is referred to the web version of this article.)

(Fig. 4b and c). Since the plasma levels of cytokines (IL-1, IL-6, etc.) were not significantly different from the baseline (Table S1), the sudden increase in blood fluorescence should be irrelevant to cytokine storms. These results suggest that the collective fluorophores increase might result from a sudden release of intracellular fluorophores after tissue damage.

2.2. Plasma fluorescence intensity depends on the injury severity

Then, for each rat, we normalized the plasma fluorescence intensities at the ischemia phase (IS) and reperfusion phase (IR) over their corresponding baseline samples to calibrate the individual variance and enhance the sensitivity of injury detection. The self-calibrated enhancement ratio (IS/BL and IR/BL) of porphyrins and flavins can report similar trends (Fig. 5b and c) to the plasma LDH level (Fig. S5). Longer ischemia duration and reperfusion after ischemia aggravate tissue damage and lead to higher plasma fluorescence. Interestingly, slight but noticeable fluorescence enhancement in the 30-minute ischemia group (O30) appeared, while the difference in LDH levels was insignificant. This performance suggests both flavin and porphyrin fluorescence intensity can reflect the severity of the intestinal injury. Considering future in vivo applications, we need a longer excitation wavelength to acquire signals from deeper vessels. The flavin fluorescence is a better choice for assessing intestinal injury.

2.3. The plasma fluorescence ratio reflects the condition of shock

Blood reperfusion after long mesenteric ischemia may lead to hypovolemic shock [24]. Extending the ischemic time to 120 min (O120), all rats had severely decreased systolic blood pressure (SBP) right after the reperfusion (Fig. S6c) and without recovery of blood pressure. The sharply reduced SBP after the reperfusion also occurred in groups O90 (Fig. S6b) and O70 (Fig. S1b), but the blood pressure in these groups gradually returned to the baseline range. We employed the shock index, which is the heart rate divided by systolic blood pressure, to evaluate the presence of hypovolemic shock [25]. The shock indices of shock rats (O120, $n = 6$) were larger than 5 (Fig. S7), which were well above the rats (SI < 3) in group O90 ($n = 6$) and group S120 ($n = 6$). Then we calculate the ratio of flavin fluorescence over blue fluorescence ($R_{f/b}$) of BL, IS, and IR samples. For each rat, we divided the $R_{f/b}$ of IS and IR by that of BL to form the self-calibrated ratio $RR_{f/b}$. We found the $RR_{f/b}$ of IS/BL had no big difference among groups O120, O90, and S120 (Fig. 4d), but $RR_{f/b}$ values of IR/BL in the shock rats were significantly lower than that of O90 and S120 (Fig. 4e) (Mann-Whitney U test with $p = 0.0328$). This result implies that the self-calibrated $RR_{f/b}$ index could be a potential indicator to reflect the occurrence of shock.

2.4. Riboflavin is responsible for the increase of flavin fluorescence

We used ultra-performance liquid chromatography with mass spectrometry (UPLC-MS) to identify the molecules contributing to the plasma flavin fluorescence. In the fluorescence-based UPLC ($\lambda_{ex} = 450$ nm and $\lambda_{em} = 520$ nm), we separated the FAD, FMN, and riboflavin standards at different elution times of 2.74, 2.91, 3.90 min (Fig. 6a). We confirmed their corresponding mass values at m/z 786.5, 457.4, 377.4, respectively (Fig. S8). We ensured the precision and accuracy of quantification in the fluorescence-based UPLC system (Table S2). In the baseline plasma, riboflavin elution time showed a prominent peak with a much stronger signal than FMN and FAD (Fig. 6 a-b). By normalizing the fluorescence intensity of metabolites, the peak value of riboflavin was kept unchanged after 70-minute ischemia and almost doubled after the following 30-minute reperfusion.

With the serial dilution of 400 nM standards, we made the standard curves of concentration versus peak area (Fig. S9). In group O70, the FAD concentration in BL, I70, and I70 + R30 plasma was fixed at around 36 nM (Fig. 6c). The FMN's concentration decreased from 47.3 ± 14.3 nM to 30.8 ± 7.4 nM after 70-minute ischemia. The FMN didn't show an apparent increase after 30-minute reperfusion (Fig. 6d). The

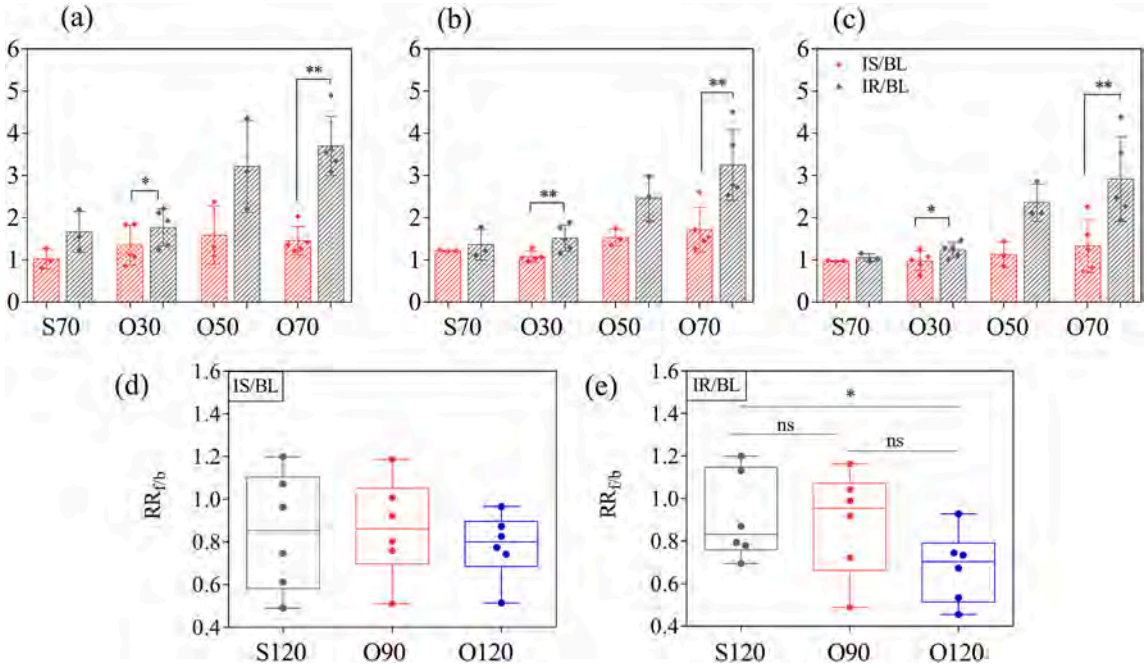

Fig. 5. Individually normalized fluorescence enhancement ratio of ischemia samples (IS/BL, red columns) and ischemia-reperfusion samples (IR/BL, gray columns) over baseline ones in the blue fluorescence (a), porphyrin fluorescence (b), and flavins fluorescence (c). Damage severities of groups O30 ($n = 5$), O50 ($n = 3$), and O70 (n = 5) were compared with that of sham group S70 (n = 3). Box plots of $RR_{f/b}$-IS/BL (d) and $RR_{f/b}$-IR/BL (e) in sham group S120 ($n = 6$), O90 (n = 6), and O120 ($n = 6$). Mann-Whitney U test is used for hypothesis testing. Statistical significance $^*p < 0.05$, $^{**}p < 0.01$; ns indicated that there was no significant difference between groups. The definition of groups is described in the Methods section. The Mann-Whitney U test couldn't be applied on O50, due to the limitation of case number (n = 3). (For interpretation of the references to color in this figure legend, the reader is referred to the web version of this article.)

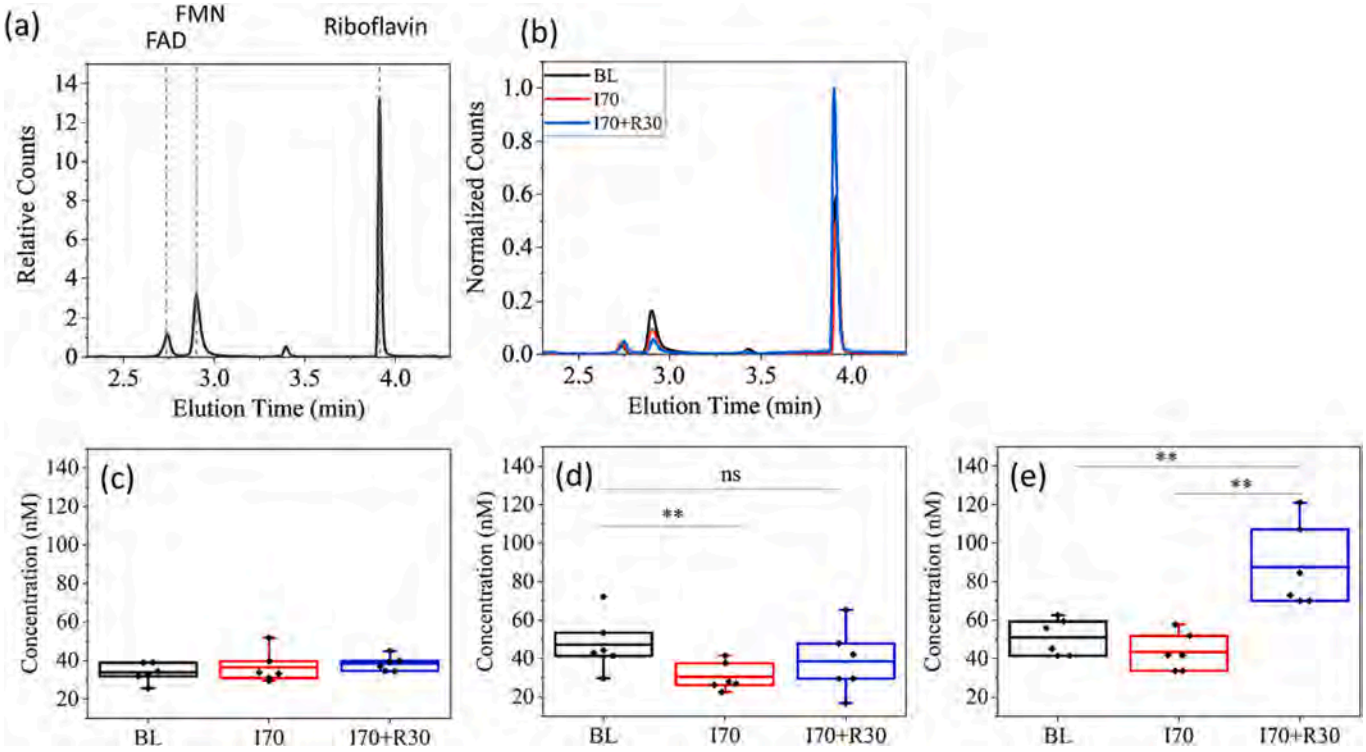

Fig. 6. (a) The UPLC elution curve of solution with mixed FAD, FMN, and riboflavin standard. (b) The UPLC elution curves of plasma samples from a rat in group O70. BL: baseline (gray); I70: ischemia for 70 min (red); I70 + R30: ischemia for 70 min and then reperfusion for 30 min (blue). The plasma concentrations of (c) FAD, (d) FMN, and (e) riboflavin were quantified by the UPLC. The plasma samples were from the rats in group O70 ($n = 6$). Mann-Whitney U test is used for significant analysis. Statistical significance $^{*}p < 0.05$, $^{**}p < 0.01$. ns indicated that there was no significant difference between groups. (For interpretation of the references to color in this figure legend, the reader is referred to the web version of this article.)

concentration of I70 plasma riboflavin was not significantly different from BL (51.2 ± 8.6 nM v.s. 42.8 ± 9.0 nM), but I70 + R30 plasma riboflavin increased substantially to 83.0 ± 23.2 nM after the following 30-minute reperfusion (Fig. 6e).

3. Discussion

The human body cannot synthesize riboflavin, and the intestinal mucosa is the only route to absorb it [26]. Since riboflavin absorption is carrier-mediated and regulated by the intestinal mucosa, once damaged by ischemia-reperfusion injury, the nutritional and commensal-derived riboflavin [27] may passively cross the dysfunction barriers and massively diffuse into blood circulation. Such dysregulated absorption could increase the level of blood riboflavin in AMI rats. As for the effects of riboflavin on the pathology of acute illness, it is worth further exploration. Many research groups have found that flavin supplements could suppress nociception [28–30], remarkedly diminish the level of inflammatory cytokines [31–34] in sepsis, inhibit the cisplatin-induced apoptosis [35], and reduce systemic oxidative stress in inflammatory bowel diseases patients [36]. Therefore, we speculate that the elevation of riboflavin concentration in plasma may play a protective role against inflammatory tissue damage in AMI.

Practically, our results demonstrate plasma fluorescence as a sensitive and rapid method to assess the severity of an intestinal injury or to report changed riboflavin metabolism in different contexts of acute illness. For instance, it may serve as an early screening indicator for deadly AMI. The early symptoms of AMI are mainly abdominal pain, distention, and vomiting, which are similar to those of other acute abdominal illnesses. It is difficult to diagnose AMI because of non-specific clinical signs. Usually, it's too late when medical doctors validate AMI with computed tomography (CT) imaging. To achieve early diagnosis, scientists proposed many serum biomarkers, including L-lactate, D-lactate, D-dimer [37], and intestinal fatty acid binding protein (I-FABP) [38]. So far, I-FABP has the best performance of 80 % pooled sensitivity and 85 % specificity [38]. Although the elevation of I-FABP concentration is the most specific hallmark among these early-stage markers, its quantification accuracy was poor and not consistent among different studies. Besides, within the same study, the individual baseline level of I-FABP varied a lot (from 533 to 1488 pg/ml) [39]. In contrast, our plasma fluorescence technique has the advantages of self-calibration and constant monitoring. If doctors have ruled out the possibility of other abdominal acute illnesses, a soaring flavin fluorescence of plasma could indicate the presence of AMI. Doctors may further confirm the diagnosis with the I-FABP level. The cooperation of plasma flavin fluorescence with I-FABP may achieve a more reliable AMI diagnosis at its early stage.

Plasma flavin fluorescence could also indicate the biochemical deficiency of riboflavin [40] in ischemic stroke patients with gastrointestinal complications [41]. Moreover, 46 % of critical illnesses are accompanied by intestinal damage due to hypoperfusion [42]. Those ICU patients with intestinal damage have a high risk of systemic inflammatory response syndrome (SIRS) and MODS. The mortality rate of these patients is 31 % higher than that of patients without intestinal injury [42]. That is because the intestine is one of the biggest immune organs and whose damage often triggers remote liver injury [43] and lung injury [44]. Moreover, by measuring plasma FAD, FMN, and riboflavin of 119 healthy subjects and 125 critically ill patients, critically ill patients had higher levels of plasma FMN and riboflavin [45]. Thus, if we have this modality to early detect latent intestinal injury, doctors could give intervention like fluid resuscitation to reduce the mortality of ICU patients.

In addition, the profile of plasma fluorophores could provide extra information about the potential risk of critical illness conditions such as shock. In this study, the plasma of shock rats showed a significantly

lower calibrated ratio $RR_{f/b}$ of flavin fluorescence over the blue fluorescence, which resulted from the increase of NADH and, thus, the decrease of $RR_{f/b}$.

Lastly, ischemic damage to other organs may also release organ-specific metabolic fluorophores. For example, plasma bilirubin, a clinical liver function index, increases in rats with hepatic ischemia-reperfusion [46]. As in our previous study, bilirubin dimer has characteristic red fluorescence in liver hepatocytes [23]. Therefore, ischemic liver damage could increase the bilirubin dimer fluorescence in plasma.

However, there are still hurdles for riboflavin fluorescence to serve as a robust marker in clinical diagnosis. Firstly, whether the elevated riboflavin level is a specific marker of intestinal mucosa injury needs further validation in other animal models and clinical studies. We need to investigate the dynamic change of blood fluorescence in other acute illnesses like sepsis or acute organ injury. Combination with serum I-FABP may achieve better specificity. Secondly, it will be more difficult to transdermally measure the vascular flavin fluorescence beneath the thick human skin. For real-time monitoring, we might need to develop an invasive blood-vessel catheterization with a fiber-optic-based fluorescence spectrometer. Based on this design, the blood fluorophores features could be evaluated in vivo without the necessity of blood sampling. In the future, this technique has a high potential to be developed as a label-free and quick screening tool for AMI, MODS, or specific organ dysfunction.

4. Materials and methods

4.1. Animals and experiment design

All the protocols were approved by the Institutional Animal Care and Use Committee of Medicine, National Taiwan University, under case number 20140147, and also approved by the Animal Research Core of the University of Macau and Ethics Committee, approved protocol ID: UMARE-024-2018. All procedures followed the guide for the care and use of laboratory animals. Male Wistar rats from BioLASCO Taiwan Co., Ltd. or Animal Research Core of the University of Macau at ages between 8 and 12 weeks, weighing 350 ± 50 g, were used in this study. The animals were kept in a facility with room temperature at 24 ± 2 °C and relative humidity at 60 ± 10 % and 12–12 h of the dark-light cycle. Reverse osmosis water and standard diet chow (LabDiet No.5010) were accessed ad libitum. To avoid the diet-induced change of blood fluorescence, all the rats underwent overnight fasting before the experiment. In our experiment design, rats were randomly divided into five operation groups and two sham control groups. For operation groups, the AMI model clamped the superior mesenteric artery (SMA) for 30, 50, 70, 90, and 120 min, followed by reperfusion for 30 min. They are denoted as O30, O50, O70, and O90, O120, respectively. The sham control groups (S70, S120) underwent laparotomy but made no clamping on SMA for 70 and 120 min, respectively.

When conducting experiments, animals were anesthetized by inhaling 5 % isoflurane at 1000 ml/min oxygen flow followed by 1–2 % at 600 ml/min oxygen flow for maintenance. A heating pad was applied to keep the core temperature at about 37 °C. The femoral artery was catheterized for blood sampling and arterial pressure measurement. For each rat, we sequentially collected blood samples (1 ml for each) at three different time points, which are the baseline sample before SMA clamping, the ischemic (IS) sample before clamp removal, and the ischemia-reperfusion (IR) sample at 30 min after clamp removal. The same volume of normal saline was infused via a femoral vein catheter after blood sampling. Blood pressure, heart rate, respiration rate, and electrocardiography (ECG) were recorded by MP45 data acquisition system (BIOPAC System Inc.) with a suitable pressure transducer and probes. After performing laparotomy by 3 to 4-cm incisions, the SMA was clamped with a bulldog clamp at the aortic bifurcation in the experimental groups. Then we closed the wounds with 3-0 surgical sutures. The sham control groups underwent laparotomy without SMA clamping. The blood sampling time points of S70 and S120 were the same as those in O70 and O120, respectively.

After the last blood sampling, the rats were euthanized under overdose carbon dioxide. Macroscopic overviews of rats were examined within 5 min after euthanasia. About 1 cm of intestinal segments was harvested and immersed into 10 % buffered formaldehyde, embedded with paraffin, cut into a 5-mm section, and stained by hematoxylin and eosin. A veterinary pathologist studied the histopathology of intestine tissues to determine the alterations caused by ischemia and reperfusion.

4.2. Plasma preparation and storage

All the blood samples were collected in tubes with heparin for anticoagulation. Rat blood plasma was prepared through double-centrifuging at 10 °C (1st run: 500 ×g for 5 min and 2nd run: 3000 ×g for 20 min) and stored at −80 °C until the completion of all of the below tests.

4.3. Biochemical assays

The enzymatic activities of lactate dehydrogenase (LDH) in blood plasma were measured by colorimetric assay kits (K726, BioVision); The kit can detect 1–100 mU/ml LDH in plasma samples. The mU/ml is defined by the amount (nmol) of NADH generated per minute per ml of the sample under the enzymatic reaction of LDH. The total Nitric Oxide (NO) in the plasma was measured by the Nitric Oxide assay kit (USA, Thermo Fisher Scientific, Cat# EMSNO). The relative levels of nitrite and nitrate in a system can vary substantially. Therefore, the most accurate determination of total NO production requires the measurement of both nitrate and nitrite.

4.4. Absorption spectra measurement

The absorption spectra of the blood plasma were taken by the spectrometer HITACHI U-3010. For each measurement, a 100 μl plasma sample was diluted with 700 μl phosphate-buffered saline (PBS), and the total 800 μl solution was filled in the quartz cuvette. The measurement ranges of the absorption spectra were 350–700 nm at a 1 nm spectral resolution.

4.5. Fluorescence spectra measurement

Single-photon fluorescence spectra of blood plasma were measured by a sensitive fluorescence spectrometer equipped with two monochromators (FLS 920, Edinburgh Instruments). The first monochromator selected the excitation wavelength from a 450 W Xenon lamp. Tuning the exit slit size, we set the line width of excitation at around 1 nm. The excitation light was focused on the cuvette, and the plasma fluorescence signals were collected in a perpendicular direction. Before entering the entrance slit of the second monochromator, we put a 420-nm (or 496-nm) long-pass filter to block the side-scattered excitation light. Then the fluorescence signal was coupled to a 0.4-mm sized entrance slit and dispersed by the grating of the second monochromator. Finally, the fluorescence intensity at each wavelength was selected by an exit slit and sequentially detected by a photomultiplier tube (PMT) cooled down to −19 °C. The resolution of fluorescence spectra measurement was 0.5 nm and the dwell time at each wavelength was 0.2 s. To calibrate the varied excitation intensity or collection efficiency in each measurement batch, we measured the Raman scattering spectrum of water corresponding to the 3400 cm^{-1} vibration mode. All the fluorescence intensities of blood plasma were normalized according to the water Raman peak. The representative intensities of blue fluorescence (Iblue), porphyrin fluorescence (Iporphyrin), and flavin fluorescence (Iflavin) were calculated from the mean spectral intensities around 440–470 nm, 610–630 nm, and 510–540 nm, respectively (Fig. 3g-i).

To real-time monitor the effects of AMI on the blood flavin

fluorescence in vivo, we used 920 nm femtosecond laser pulses to perform multiphoton angiography imaging in a rat's ear. At a 30 Hz frame rate, we could locate the vessels from the flowing red blood cells carrying the two-photon flavin fluorescence. Then we took the time-course two-photon fluorescence image of blood plasma and blood cells every 30 s. At the same time, the rat underwent the 70 min ischemia-reperfusion procedure. We recorded the time-course multiphoton images from the 50th-minute post-SMA ligation to the endpoint of reperfusion.

4.6. Chromatography analysis

The UPLC-FLR-MASS analysis was performed by a WATERS Xevo TQD triple-quadrupole mass spectrometer coupled with an ACQUITY UPLC H-class system and an FLR fluorescence detector (Waters, USA). Compounds were separated on ACQUITY BEH C18 column (100 × 2.1 mm) containing 1.7 μm particles (Waters, USA) with a VanGuard. Chromatographic separations were performed by using a binary gradient mobile phase composed of mobile phase A (3.85 g/l Ammonium Acetate in distilled water) and mobile phase B (3.85 g/l Ammonium Acetate in Water/Acetonitrile 7:3(v/v)). The gradient program for the UPLC-FLR was as follows: 0–2 min, 20–40 % B; 2–3 min 40–99 % B; 3–3.5 min 99–99 % B; 3.5–4.5 min 99–20 % B, 4.5-6 min 20–20 %, and the flow rate was 0.4 ml/min. The injection volume was 10 μl. The column oven temperature was set at 40 °C, and the total run time was 6.0 min. The ionization mode is ES+, and a mass spectrum in the *m/z* range of 100–1500 was obtained. The FAD, FMN, and Riboflavin were detected by an FLR detector with an excitation wavelength of 450 nm and an emission wavelength of 520 nm.

4.7. Data statistics

All scale bars are presented as mean ± SD unless indicated. A four-parameter algorithm provides the best standard curve fit for biochemical and ELISA detection. Mann-Whitney *U* test was used for significant analysis, and the level of significance was set at $p \leq 0.05$.

Supplementary data to this article can be found online at https://doi.org/10.1016/j.thromres.2023.01.032.

Credit authorship contribution statement

Conceptualization and Experiment Design: HCT, YHC, CLL, PTC, IRL, TML.
Animal Study: XQW, LZG, YHL, YCL, CHL, CLL.
Spectra Measurement: XQW, YSL, LZG, PLY.
Biochemical Assay: XQW, YHL, JCWL, CHL.
HPLC Performance: XQW, YSL,
Histopathology: CHL.
Data Process: XQW, LZG, TDW.
Writing: XQW, LZG.
Funding: TML, CLL.

Declaration of competing interest

The concept of this work has filed an application of a United States patent with the University of Macau as the assignee. This patent application is pending with publication number US20200093415A1.

Acknowledgments

Thanks for the following funding for science research:

Multi-Year Research Grant of University of Macau MYRG2018-00070-FHS (TML)
The Macao Science and Technology Development Fund 122/2016/A3 (TML)
The Macao Science and Technology Development Fund 018/2017/A1 (TML)
The Macao Science and Technology Development Fund 0011/2019/AKP (TML)
The Macao Science and Technology Development Fund 0120/2020/A3 (TML)
The Macao Science and Technology Development Fund 0026/2021/A (TML)
National Taiwan University Hospital Hsin-Chu Branch Fund 110-HCH-012 (CLL)
National Taiwan University Hospital Hsin-Chu Branch Fund 110-HCH-092 (CLL)
Ministry of Science and Technology of Taiwan Fund MOST 110-2320-B-002-042 (CLL).

References

[1] D.C. Fajgenbaum, C.H. June, Cytokine storm, N. Engl. J. Med. 383 (2020) 2255–2273.
[2] S.W. Park, M. Kim, K.M. Brown, V.D. D'Agati, H.T. Lee, Paneth cell-derived interleukin-17A causes multiorgan dysfunction after hepatic ischemia and reperfusion injury, Hepatology 53 (2011) 1662–1675.
[3] R.S. Hotchkiss, et al., Sepsis and septic shock, Nat. Rev. Dis. Primers 2 (2016) 16045.
[4] J.L. Vincent, et al., The SOFA (Sepsis-related Organ Failure Assessment) score to describe organ dysfunction/failure. On behalf of the Working Group on Sepsis-related Problems of the European Society of Intensive Care Medicine, Intensive Care Med. 22 (1996) 707–710.
[5] C. Lelubre, J.L. Vincent, Mechanisms and treatment of organ failure in sepsis, Nat. Rev. Nephrol. 14 (2018) 417–427.
[6] D.N. Granger, P.D. Richardson, P.R. Kvietys, N.A. Mortillaro, Intestinal blood flow, Gastroenterology 78 (1980) 837–863.
[7] M. Meng, N.J. Klingensmith, C.M. Coopersmith, New insights into the gut as the driver of critical illness and organ failure, Curr. Opin. Crit. Care 23 (2017) 143–148.
[8] C.J. Doig, et al., Increased intestinal permeability is associated with the development of multiple organ dysfunction syndrome in critically ill ICU patients, Am. J. Respir. Crit. Care Med. 158 (1998) 444–451.
[9] S. Otani, C.M. Coopersmith, Gut integrity in critical illness, J. Intensive Care 7 (2019) 17.
[10] L.N. Segal, et al., Enrichment of the lung microbiome with oral taxa is associated with lung inflammation of a Th17 phenotype, Nat. Microbiol. 1 (2016) 16031.
[11] K.T. Fay, M.L. Ford, C.M. Coopersmith, The intestinal microenvironment in sepsis, Biochim. Biophys. Acta Mol. basis Dis. 1863 (2017) 2574–2583.
[12] F. Haussner, S. Chakraborty, R. Halbgebauer, M. Huber-Lang, Challenge to the intestinal mucosa during sepsis, Front. Immunol. 10 (2019) 891.
[13] B.W. Haak, W.J. Wiersinga, The role of the gut microbiota in sepsis, Lancet Gastroenterol. Hepatol. 2 (2017) 135–143.
[14] D.G. Clair, J.M. Beach, Mesenteric ischemia, N. Engl. J. Med. 374 (2016) 959–968.
[15] J.M. Kärkkäinen, Acute mesenteric ischemia: a challenge for the acute care surgeon, Scand. J. Surg. 110 (2021) 150–158.
[16] M. Bala, et al., Acute mesenteric ischemia: updated guidelines of the World Society of Emergency Surgery, World J. Emerg. Surg. 17 (2022) 54.
[17] S.F. Assimakopoulos, et al., Gut-origin sepsis in the critically ill patient: pathophysiology and treatment, Infection 46 (2018) 751–760.
[18] J.T. Pinto, J. Zempleni, Riboflavin, Adv. Nutr. 7 (2016) 973–975.
[19] K. Yoshii, K. Hosomi, K. Sawane, J. Kunisawa, Metabolism of dietary and microbial vitamin B family in the regulation of host immunity, Front. Nutr. 6 (2019) 48.
[20] S.Y. Seong, P. Matzinger, Hydrophobicity: an ancient damage-associated molecular pattern that initiates innate immune responses, Nat. Rev. Immunol. 4 (2004) 469–478.
[21] A.A. Lamola, J. Eisinger, W.E. Blumberg, S.C. Patel, J. Flores, Flurorometric study of the partition of bilirubin among blood components: basis for rapid microassays of bilirubin and bilirubin binding capacity in whole blood, Anal. Biochem. 100 (1979) 25–42.
[22] J. Galbán, I. Sanz-Vicente, J. Navarro, S. de Marcos, The intrinsic fluorescence of FAD and its application in analytical chemistry: a review, Methods Appl. Fluoresc. 4 (2016), 042005.
[23] Y.F. Shen, et al., Imaging endogenous bilirubins with two-photon fluorescence of bilirubin dimers, Anal. Chem. 87 (2015) 7575–7582.
[24] R.H. Turnage, K.S. Guice, K.T. Oldham, The effects of hypovolemia on multiple organ injury following intestinal reperfusion, Shock 1 (1994) 408–412.
[25] M.Y. Rady, H.A. Smithline, H. Blake, R. Nowak, E. Rivers, A comparison of the shock index and conventional vital signs to identify acute, critical illness in the emergency department, Ann. Emerg. Med. 24 (1994) 685–690.
[26] H.M. Middleton 3rd, Uptake of riboflavin by rat intestinal mucosa in vitro, J. Nutr. 120 (1990) 588–593.
[27] L.A. Averianova, L.A. Balabanova, O.M. Son, A.B. Podvolotskaya, L.A. Tekutyeva, Production of vitamin B2 (riboflavin) by microorganisms: an overview, Front. Bioeng. Biotechnol. 8 (2020), 570828.

[28] C.M. Bertollo, et al., Characterization of the antinociceptive and anti-inflammatory activities of riboflavin in different experimental models, Eur. J. Pharmacol. 547 (2006) 184–191.
[29] D.S. França, et al., B vitamins induce an antinociceptive effect in the acetic acid and formaldehyde models of nociception in mice, Eur. J. Pharmacol. 421 (2001) 157–164.
[30] V. Granados-Soto, et al., Riboflavin reduces hyperalgesia and inflammation but not tactile allodynia in the rat, Eur. J. Pharmacol. 492 (2004) 35–40.
[31] T. Toyosawa, M. Suzuki, K. Kodama, S. Araki, Effects of intravenous infusion of highly purified vitamin B2 on lipopolysaccharide-induced shock and bacterial infection in mice, Eur. J. Pharmacol. 492 (2004) 273–280.
[32] A.I. Mazur-Bialy, E. Pocheć, HMGB1 inhibition during zymosan-induced inflammation: the potential therapeutic action of riboflavin, Arch. Immunol. Ther. Exp. 64 (2016) 171–176.
[33] S. Dey, B. Bishayi, Riboflavin along with antibiotics balances reactive oxygen species and inflammatory cytokines and controls Staphylococcus aureus infection by boosting murine macrophage function and regulates inflammation, J. Inflamm. 13 (2016) 1–21.
[34] T. Toyosawa, M. Suzuki, K. Kodama, S. Araki, Highly purified vitamin B2 presents a promising therapeutic strategy for sepsis and septic shock, Infect. Immun. 72 (2004) 1820–1823.
[35] I. Hassan, S. Chibber, I. Naseem, Vitamin B2: a promising adjuvant in cisplatin based chemoradiotherapy by cellular redox management, Food Chem. Toxicol. 59 (2013) 715–723.
[36] J.Z.H. von Martels, et al., Riboflavin supplementation in patients with Crohn's disease [the RISE-UP study], J. Crohns Colitis 14 (2020) 595–607.
[37] M. Montagnana, E. Danese, G. Lippi, Biochemical markers of acute intestinal ischemia: possibilities and limitations, Ann. Transl. Med. 6 (2018) 341.
[38] D.L. Sun, et al., Accuracy of the serum intestinal fatty-acid-binding protein for diagnosis of acute intestinal ischemia: a meta-analysis, Sci. Rep. 6 (2016) 34371.
[39] T. Kitai, et al., Circulating intestinal fatty acid-binding protein (I-FABP) levels in acute decompensated heart failure, Clin. Biochem. 50 (2017) 491–495.
[40] S. Gariballa, R. Ullegaddi, Riboflavin status in acute ischaemic stroke, Eur. J. Clin. Nutr. 61 (2007) 1237–1240.
[41] S. Kumar, M.H. Selim, L.R. Caplan, Medical complications after stroke, Lancet Neurol. 9 (2010) 105–118.
[42] H. Chen, H. Zhang, W. Li, S. Wu, W. Wang, Acute gastrointestinal injury in the intensive care unit: a retrospective study, Ther. Clin. Risk Manag. 11 (2015) 1523–1529.
[43] S. Wen, et al., HMGB1-associated necroptosis and Kupffer cells M1 polarization underlies remote liver injury induced by intestinal ischemia/reperfusion in rats, FASEB J. 34 (2020) 4384–4402.
[44] G. Li, Y. Zhang, Z. Fan, Cellular signal transduction pathways involved in acute lung injury induced by intestinal ischemia-reperfusion, Oxidative Med. Cell. Longev. 2021 (2021) 9985701.
[45] A.T. Vasilaki, et al., Relation between riboflavin, flavin mononucleotide and flavin adenine dinucleotide concentrations in plasma and red cells in patients with critical illness, Clin. Chim. Acta 411 (2010) 1750–1755.
[46] W. de Graaf, et al., Quantitative assessment of liver function after ischemia-reperfusion injury and partial hepatectomy in rats, J. Surg. Res. 172 (2012) 85–94.